

An Iterative Algorithm Based on the Measured Equation of Invariance for the Scattering Analysis of Arbitrary Multicylinders

Jun Chen and Wei Hong, *Member, IEEE*

Abstract— It is known that the measured equation of invariance (MEI) is generally valid for outgoing waves just as other absorbing boundary conditions (ABC's). However, for the scattering problem of multicylinders, the scattered field from one cylinder is just the in-going incident wave to other cylinders. So the MEI cannot be directly applied to the scattering problem of multicylinders. In this paper, an iterative algorithm based on the MEI is first proposed for the scattering problems of multicylinders with arbitrary geometry and physical parameters. Each cylinder is coated with several layers of meshes and the MEI's are applied to the truncated mesh boundaries. It has been demonstrated that the MEI can truncate the meshes very close to the surfaces of the cylinders and then results in dramatically savings in memory requirements and computational time. The MEI coefficients of each cylinder can be stored and reused to form the sparse matrices during each iteration procedure as they are independent of excitations. So more central processing unit (CPU) time is saved as the MEI coefficients are calculated only once in the algorithm. The method can be applied to problems of various kinds of multiple cylinders with arbitrary configurations and cross sections. Numerical results for the scattered fields are in good agreement with the data available. Finally, examples are given to show the iterative algorithm applicable to electrically large multicylinders coated with lossy media.

Index Terms— Iterative algorithm, measured equation of invariance, multiple scattering.

I. INTRODUCTION

THE multiple scattering of a plane wave by a system of N cylinders is important in a variety of practical applications. For instance, the solution can be used to study the propagation of electromagnetic waves through a city where complex skyscrapers can be modeled by a collection of cylinders.

The scattering by conducting cylinders of arbitrary cross section was investigated by Twersky in 1952 [1], who gave the total field as an incident field plus scattered fields of various orders generated by an iterative procedure and later expressed the multiple-scattering solution as a series of Hankel function of the single-scattering cylinder. The formula is valid when

the separation is large compared to the cylinder. Since then, many researchers made attempts to deal with more practical configurations with kinds of methods [2]–[9]. For example, Elsherbeni and Hamid [7] coped with cylinders of arbitrary cross section and spacing between cylinders approaching zero. However, little effect is made to handle with other kind of cylinders except conducting ones. The reason is explicitly that the existing field solution of a single conducting cylinder enables the solution of multiple scattering simple whatever the method is, which, therefore, is naturally believed to illustrate the method effectively. Although a complex multicylinder system is, say, not within a restriction of the presented method theoretically, no example and data are available for complex media, i.e., inhomogeneous dielectric or lossy coated conducting cylinder. In fact, complicated geometry and complex media often make it impossible to complete the formula deduction and require a large executive time to achieve a good accuracy by these methods.

In the present paper, we attempt to cover a wide range of multiple scattering problem by a novel iterative algorithm based on measured equation of invariance, which involves a system of conducting cylinders with arbitrary cross sections, a system of inhomogeneous dielectric cylinders with arbitrary cross sections, and a system of arbitrarily shaped conducting cylinders coated with lossy inhomogeneous dielectric media. The benefit of this presented method is that arbitrary geometry and complex media are well rendered in the finite-difference (FD) equation deduced. Thus, the effects by discontinuity and inhomogeneity and so on are easily involved for a complicated system.

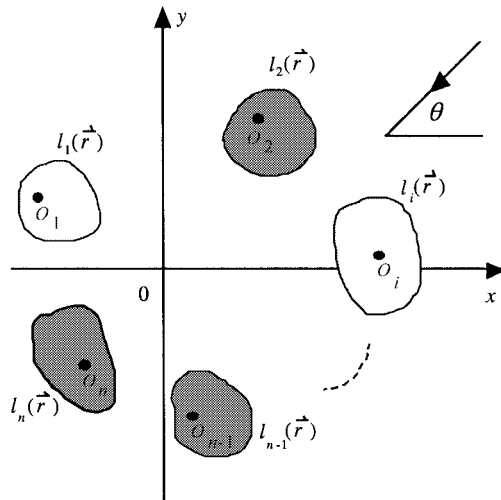
The FD once was regarded as a memory-consuming method in comparison with the boundary methods, because the truncation boundary should be far from the scattering surface if conventional absorbing boundary conditions (ABC's) are used [10]. So less literature combines the iteration procedure with the FD method. Fortunately, the measured equation of invariance (MEI), presented in 1994 [11], is able to truncate the boundary much closer to the surface. This new technique has been successfully applied to various electromagnetic (EM) problems [12]–[15]. In this paper, the measured equation of invariance (MEI) method is first used to the iterative procedure for the multiscattering problem. The invariance characteristic is made full use of during the iterations, which means the MEI coefficients for each node at the truncation may not change

Manuscript received April 4, 1996; revised July 31, 1996.

J. Chen is with Computer Engineering Department, University of California, Santa Cruz, CA 95064 USA.

W. Hong is with State Key Laboratory of Millimeter Waves, Department of Radio Engineering, Southeast University, Nanjing, 210096 China.

Publisher Item Identifier S 0018-926X(99)07076-3.

Fig. 1. Scheme of multiple scattering by N cylinders.

as they are invariant to different excitations, thus, they are calculated only once and can be stored and reused. Details will be presented in the following sections.

II. FORMULA

Consider N parallel infinitely long circular cylinders as shown in Fig. 1. These cylinders are situated such that their axes are parallel to the z axis of the global coordinate system. Each cylinder has its own local coordinate whose original is located at $O_i(x, y)$ in the global coordinate. Cross sections of cylinders are described by curve $l_i(\vec{r})$, where \vec{r} is the local vector. These curves are useful when conformal meshes are made around cylinders. As there is no discontinuity occurring along the z axis, TM (or TE) polarized wave can exist in the system. Denoting the longitude component of the field by φ , one can write an incident plane wave of the form

$$\varphi^{\text{inc}} = e^{j k_0 (x \cos \theta + y \sin \theta)}. \quad (1)$$

And the Helmholtz equation holds in the system

$$\nabla^2 \varphi + k_0^2 \varphi = 0. \quad (2)$$

A. Measured Equation of Invariance

The concept of MEI is very important and basic for the iterative (IA)-MEI. Therefore, the method should be briefly presented. The problem dealt with in the paper involves complex media, so the technique to decouple the electric metrons and the magnetic metrons, which is first presented in [12], is necessarily applied. The node configuration for MEI is shown in Fig. 1 and the MEI may be represented by a local linear equation of the type

$$\sum_{i=1}^4 c_i \phi_i^s = 0 \quad (3)$$

where c_i are the MEI coefficients and will be determined by *metrons*, which are defined on the scattering surface; the superscript “ s ” stands for scattered field.

For the general case, both the equivalent electric current $J_e(\vec{r}')$ and magnetic current $M_e(\vec{r}')$ exist on the surface, so the scattered field is

$$\begin{aligned} \phi^s(\vec{r}_i) = & - \int_{\Gamma} \left[M_e(\vec{r}') \frac{\partial}{\partial n'} G(\vec{r}_i, \vec{r}') \right. \\ & \left. + j\omega\mu_0 J_e(\vec{r}') G(\vec{r}_i, \vec{r}') \right] dl' \quad (\text{TM wave}) \end{aligned} \quad (4)$$

$$\begin{aligned} \phi^s(\vec{r}_i) = & \int_{\Gamma} \left[\eta_0 J_e(\vec{r}') \frac{\partial}{\partial n'} G(\vec{r}_i, \vec{r}') \right. \\ & \left. - jk_0 M_e(\vec{r}') G(\vec{r}_i, \vec{r}') \right] dl' \quad (\text{TE wave}) \end{aligned} \quad (5)$$

where \vec{r}_i are the position vectors of MEI nodes, \vec{r}' the position vectors on the surface, and n' the outward normal direction of the surface. $G(\vec{r}_i, \vec{r}')$ is the Green's function of free-space, $G(\vec{r}_i, \vec{r}') = -j/4H_0^{[2]}(k_0|\vec{r}_i - \vec{r}'|)$, and $H_0^{[2]}(*)$ is the Hankel function of the second kind.

Usually, the metrons may be chosen as

$$\psi(l') = \begin{cases} \cos(2\pi nl'/L) & n = 0, 1, 2, \dots \\ \sin(2\pi nl'/L) & \end{cases} \quad (6)$$

where L is the circumferential length of the cylinder.

In (4) or (5), the scattered field produced by the metrons corresponding to the equivalent electric current and the equivalent magnetic current is not independent. To decouple these two fields, a simple decomposition technique is used by considering that

$$\phi^s = \phi^e + \phi^m \quad (7)$$

where

$$\phi_{ni}^e(\vec{r}_i) = \int_{\Gamma} \psi_n(l') D_e G(\vec{r}_i, \vec{r}') dl' \quad (8)$$

$$\phi_{ni}^m(\vec{r}_i) = \int_{\Gamma} \psi_n(l') D_m G(\vec{r}_i, \vec{r}') dl' \quad (9)$$

and

$$D_e = \begin{cases} 1 & (\text{TM}) \\ \partial/\partial n' & (\text{TE}), \end{cases} \quad D_m = \begin{cases} \partial/\partial n' & (\text{TM}) \\ 1 & (\text{TE}). \end{cases} \quad (10)$$

Substituting the scattered fields ϕ^e and ϕ^m produced by electric and magnetic metrons into MEI, respectively, yields

$$\sum_{i=1}^4 c_i \phi_{ni}^e(\vec{r}_i) = 0 \quad n = 1, 2, \dots, M \quad (11)$$

$$\sum_{i=1}^4 c_i \phi_{ni}^m(\vec{r}_i) = 0 \quad n = 1, 2, \dots, M. \quad (12)$$

It is easy to understand that if the MEI is valid for electric and magnetic metrons separately, it should be valid for any combinations of electric and magnetic metrons due to the homogeneity of MEI. Solving the system of linear algebraic (11) and (12) simultaneously, we obtain the MEI coefficients c_i .

B. Finite-Difference Equation and Scattered Field

Conformal meshes are made around cylinder with dielectric coating. For the interior nodes, five-point FD equations are necessarily applied

$$\sum_{i=1}^5 b_i \varphi_i = 0 \quad (13)$$

where formulas for b_i are presented in [9].

Equations (3) and (13) can be used to form a sparse matrix equation. However, it should be noticed that the field in (3) is the scattered field while that in (13) is the total field. So it is necessary to split the fields for different demands. We choose the layer next to the truncated boundary as the splitting loop to achieve the separation. Field in the area closed by the splitting loop is the total field and that in the area outside the loop is scattered field. Nodes of scattered field are denoted by open circle dots while those of total field are marked by solid ones in Fig. 2. With the relation among the total field, incident field, and scattered field, which is

$$\varphi = \varphi^{\text{inc}} + \varphi^s \quad (14)$$

field of nodes on the splitting loop has the FD equation of the form

$$b_1 \varphi_1^s + b_2 \varphi_2 + b_3 \varphi_3 + b_4 \varphi_4 + b_5 \varphi_5 = -b_1 \varphi_1^{\text{inc}} \quad (15)$$

and (3) is written as

$$c_5 \varphi_5 + c_6 \varphi_6 + c_7 \varphi_7 + c_1 \varphi_1^s = c_5 \varphi_5^{\text{inc}}. \quad (16)$$

Thus, in the whole computational area the matrix equation is formed

$$[S] \bar{\Phi} = \bar{f} \quad (17)$$

where $[S]$ is a sparse matrix filled by (13), (15), and (16), $\bar{\Phi}$ is a column matrix and consists of the scattered field values φ^s at truncation nodes and the total field values φ at interior nodes, $[S] \bar{\Phi} = \bar{f}$ is a given column matrix obtained by the right side of (15) and (16) when the incident field is introduced. If $\det[S] \neq 0$, then we have $\bar{\Phi} = [S]^{-1} \bar{f}$. The equivalent electric and magnetic currents are then calculated according to the solution. Finally, the scattered fields are calculated from the equivalent currents based on (4) and (5), which, in terms of operator matrix, is

$$\bar{\Phi}^s = [A] \bar{f}. \quad (18)$$

C. Iteration Procedure

In a multicylinder system, discretization of the whole area will make the computer source inefficient. Therefore, local discretization in the local coordinate is employed. In accordance with the infinite scattering among cylinders, iterative procedure may be considered the most logical approach to determine the scattered field by multiple cylinders.

Usually, the iteration procedure assumes each cylinder to be alone in the incident field, which does not take change until the next iteration. Therefore, the first-order scattered field comes from the excitation of each cylinder by the incident

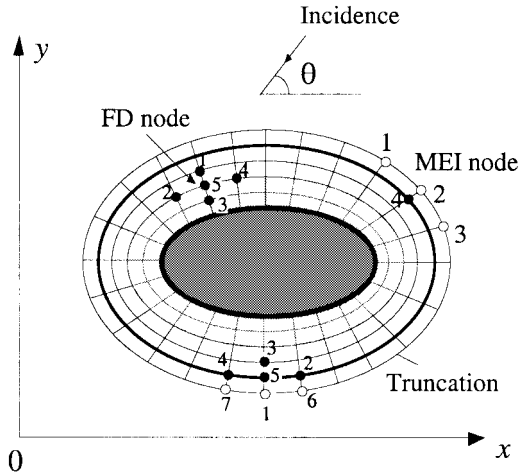


Fig. 2. FD nodes, MEI nodes with scattered (on white nodes), and total (on black nodes) fields.

plane wave only, while the second-order scattered field results from the excitation of each cylinder by the sum of all first-order scattered fields. Hence, this iterative process continues until the solution converges. That is

$$\bar{f}^{(k+1)} = \bar{\Phi}^{\text{inc}} + \sum_{i=1}^N \Phi_i^s. \quad (19)$$

From (18), the scattered field for the i th cylinder in the k th iteration is

$$\Phi_i^s = [A_i] \bar{f}^{(k)} \quad (20)$$

where $[A_i]$ represents the operator matrix for the i th cylinder. So (19) is rewritten as

$$\bar{f}^{(k+1)} = [\tilde{A}] \bar{f}^{(k)} + \bar{\Phi}^{\text{inc}} \quad (21)$$

in which

$$[\tilde{A}] = \sum_{i=1}^N [A_i]. \quad (22)$$

Equation (21) is the iterative procedure in form of matrix equation. As it is similar for this iterative process to the idea of the Jacobi algorithm for solving matrix equation, we call it the Jacobi iteration.

A further look at the Jacobi iteration finds that scattered fields of $\bar{\Phi}_1^s$, $\bar{\Phi}_2^s$, and $\bar{\Phi}_{i-1}^s$ have already been calculated and remained unused when the scattered field for the i th under $\bar{\Phi}_i^s$ is to be calculated. It is easy to see that if the incident field is modulated in time with these computed scattered fields, the convergence can be possibly sped up. So we justify the incident field for these N cylinders in the k th iteration by instantly considering the effect of scattered fields. So the scattered field for the first cylinder is

$$\bar{\Phi}_1^s = [A_1] \bar{f}^{(k)}. \quad (23)$$

And taking into consideration the effect by the first scattered field, the second cylinder has its scattered field as

$$\bar{\Phi}_2^s = [A_2] (\bar{f}^{(k)} + \bar{\Phi}_1^s). \quad (24)$$

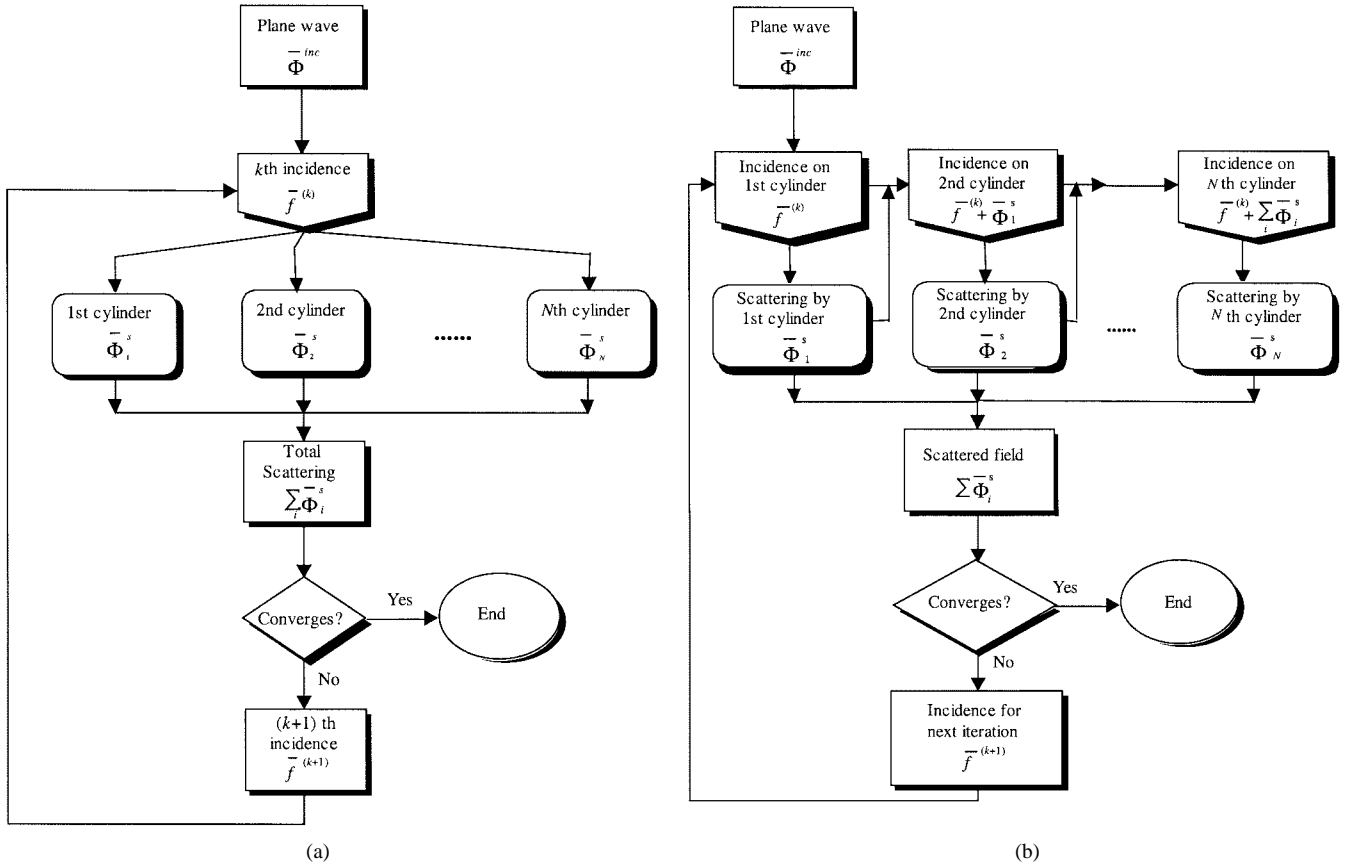


Fig. 3. Two iterative procedures based on MEI. (a) Jacobi iteration. (b) Gauss–Seidel iteration.

Similarly, scattered field for the i th cylinder is

$$\bar{\Phi}_i^s = [A_i] \left(\bar{f}^{(k)} + \sum_{j=1}^{i-1} \bar{\Phi}_j^s \right). \quad (25)$$

Substitution of (25) into (19), yields

$$\bar{f}^{(k+1)} = [D] \bar{f}^{(k)} + \bar{\Phi}^{\text{inc}} \quad (26)$$

where

$$[D] = \sum_{j=1}^N \left(\left(\sum_{i=j}^N [G_{ij}] \right) [A_j] \right) \quad (27)$$

and $[G_{ij}]$ is given by

$$\begin{cases} [G_{ii}] = [I] & (i = 1, 2, \dots, N) \\ [G_{ij}] = [A_i] \sum_{k=j}^{i-1} [G_{kj}] & (j = 1, 2, \dots, N-1) \\ & i = j+1, j+2, \dots, N \end{cases} \quad (28)$$

in which $[I]$ is the unit matrix. This iterative process is called the Gauss–Seidel iteration. Difference between these two iterations is shown in Fig. 3.

The IA-MEI described above makes full use of the concept of the MEI. Once the MEI coefficients for each cylinder have been calculated during the first iteration, in response to the idea of MEI, calculation of these coefficients does not need repeating during the following iterations. Therefore, the IA-MEI does not introduce extra computer burden.

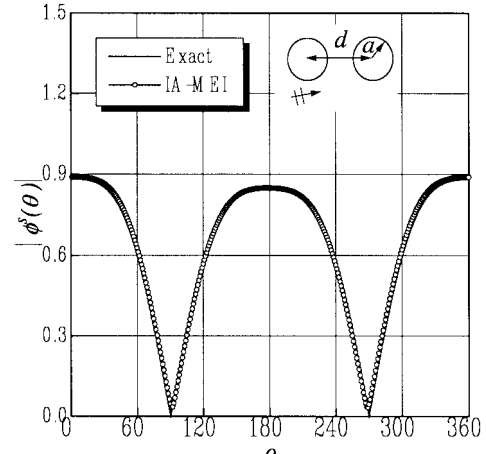


Fig. 4. Scattering pattern by two cylinders ($ka = 0.1$, $kd = 3$, $\alpha = 10^\circ$).

III. NUMERICAL RESULTS

The scattering by multiple circular cylinders is calculated and shown in Figs. 4–7. The radii of the cylinders are considered equal according to the configuration in [6].

Fig. 4 shows the scattered field for $ka = 0.1$, while the separation between the centers of the two cylinders is $kd = 3$ and the incident angle $\alpha = 10^\circ$. Fig. 5 presents the scattering patterns based on the exact and the IA-MEI method for an equispaced linear array of three cylinders. The radius and the separation between the successive cylinders are $ka = 0.75$ and

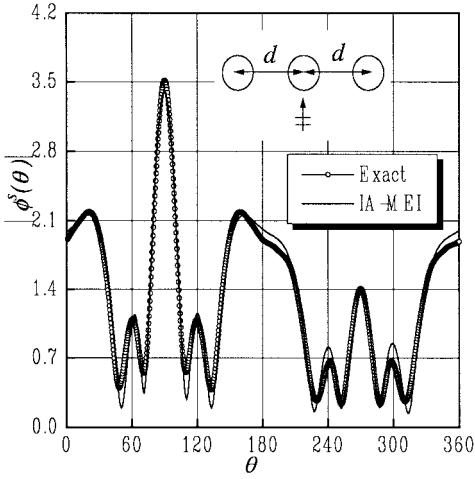


Fig. 5. Scattering patterns by three cylinders ($ka = 0.75$, $kd = 2\pi$, $\alpha = 90^\circ$).

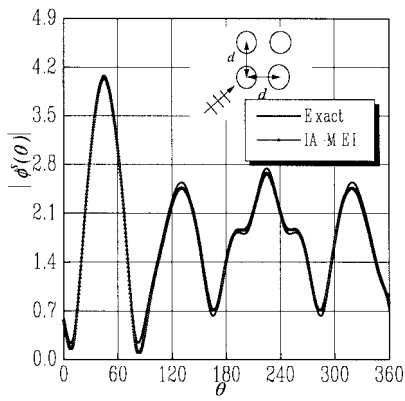


Fig. 6. Scattering pattern by four cylinders ($ka = 0.5$, $kd = 2\pi$, $\alpha = 45^\circ$).

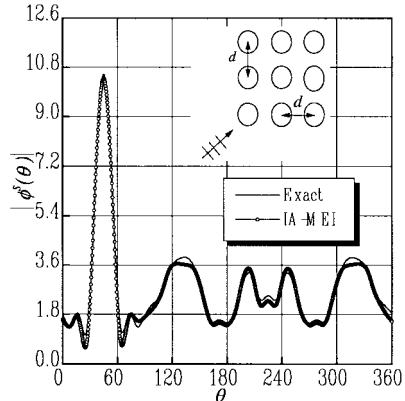


Fig. 7. Scattering patterns by nine cylinders ($ka = 0.5$, $kd = 2\pi$, $\alpha = 45^\circ$).

$kd = 2\pi$, respectively, while the incidence angle is $\alpha = 90^\circ$. The scattering pattern of a four-cylinder array located at the vertices of a square, which has side length $kd = 2\pi$ is depicted in Fig. 6. The radius of each cylinder is $ka = 0.5$, while the angle of incidence is $\alpha = 45^\circ$. Another two-dimensional (2-D) array of nine cylinders is calculated and shown in Fig. 7. The vertical and horizontal separations between the two successive cylinders are $kd = 2\pi$ with the radius $ka = 0.5$ and the

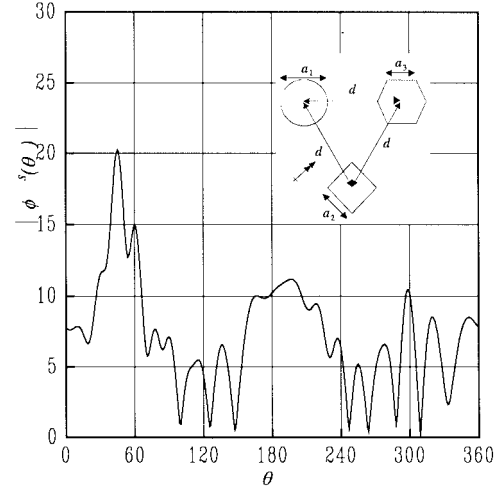


Fig. 8. Scattering pattern of three cylinders ($a_1 = 2.0\lambda$, $a_2 = 1.5\lambda$, $a_3 = 1.0\lambda$, $d = 2.0\lambda$, $\alpha = 45^\circ$).

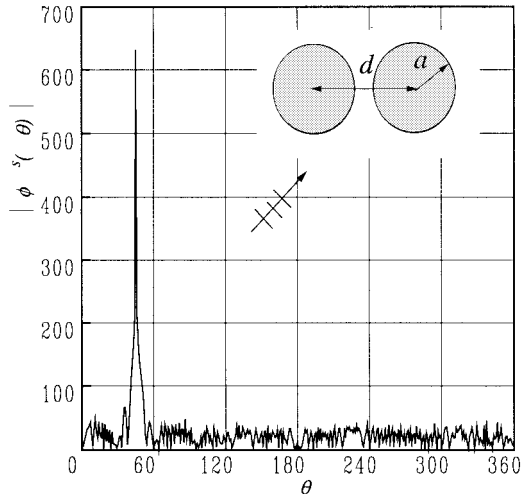


Fig. 9. Pattern of two electrically large cylinder ($a = 20.0\lambda$, $d = 50.0\lambda$, $\alpha = 45^\circ$).

incident angle $\alpha = 45^\circ$. It is easy to find good agreement between the results given by the exact solution and those by this method.

The case of three cylinders of a 2-D array is calculated. The geometry centers of the three cylinders are located at the vertices of an equilength triangular whose side length is 2.0λ . The cross sections of cylinders are shaped by a circular, a square, and a hexagon with the diameter $a_1 = 1.0\lambda$ and the side length $a_2 = 1.5\lambda$ and $a_3 = 1.0\lambda$, respectively. The incidence angle is $\alpha = 45^\circ$. Scattering pattern is shown in Fig. 8.

Then the scattering pattern of two electrically large circular cylinders is computed and shown in Fig. 9. The radii are equal, which is $a = 20\lambda$, and the separation is $d = 50\lambda$, the incidence angle $\alpha = 45^\circ$.

The scattering by two electrically large circular conducting cylinders with coating is plotted in Fig. 10. The conducting parts of the coated cylinders are the same as those in Fig. 9. So it is with the separation. The left cylinder has its dielectric coating changing along the periphery, four equal parts with

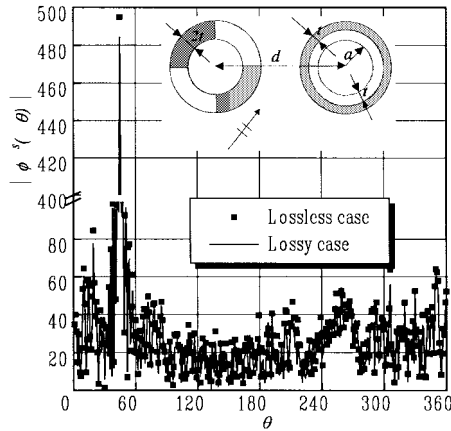


Fig. 10. Pattern of two electrically large cylinder with coating ($a = 20.0\lambda$, $d = 50.0\lambda$, $t = 0.2\lambda$, $\alpha = 45^\circ$).

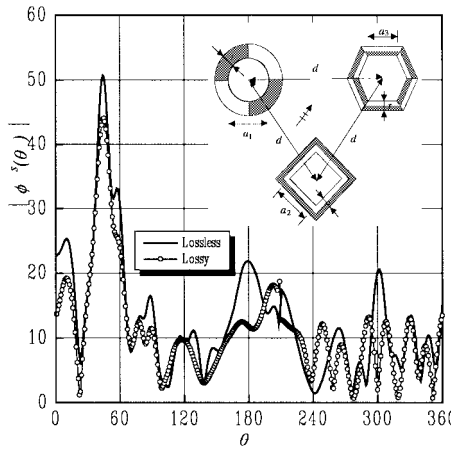


Fig. 11. Scattering pattern for three conducting circular conducting cylinders with coating ($a_1 = 2.0\lambda$, $a_2 = 1.5\lambda$, $a_3 = 1.0\lambda$, $t = 0.5\lambda$, $d = 2.0\lambda$, $\alpha = 45^\circ$).

two interval parameters. The right one has its dielectric coating changing along the radial, two layers of equal thickness with two parameters. Both the coating thicknesses of the two cylinders are equal to 0.4λ . For the case of lossless coating, the parameters are $\epsilon_{r1} = 4.0$, $\mu_{r1} = 4.0$, $\epsilon_{r2} = 2.0$, $\mu_{r2} = 2.0$. For the case of lossy coating, the parameters are $\epsilon_{r1} = 4 - 2j$, $\mu_{r1} = 4.0$, $\epsilon_{r2} = 2 - j$, $\mu_{r2} = 2.0$. The angle of incidence is $\alpha = 45^\circ$.

Finally, the scattering field of three conducting cylinders with inhomogeneous dielectric coating is depicted in Fig. 11. Both the cases of lossless and lossy coating are calculated. The size, the location and the cross section of the conducting part of the cylinders are the same as those in Fig. 8. The coating for each conducting cylinder is 0.5λ thick. Dielectric coating for the circular cylinder is divided into four equal segments along the periphery, filled at intervals by two kinds of material ϵ_{r1}, μ_{r1} (dark gray in the figure) and ϵ_{r2}, μ_{r2} (light gray in the figure). The square cylinder has its coating made up of two dielectric layers, each of which has the same dimension in thickness. The constitutive parameters for the two layers are ϵ_{r1}, μ_{r1} and ϵ_{r2}, μ_{r2} , respectively. The hexagon cylinder has its coating changed in two directions,

namely circumference and radial. The dielectric coating is segmented into twelve parts, two layers outside each board of the hexagon. Two types of material are distributed in such a manner that the neighboring segments are made sure to have different parameters. To compute the scattered field of the three-coating-cylinder system, parameters for lossless media are of the values that $\epsilon_{r1} = 4.0$, $\mu_{r1} = 1.0$, $\epsilon_{r2} = 2.0$, $\mu_{r2} = 1.0$, and for lossy media the parameters are $\epsilon_{r1} = 4 - 2j$, $\mu_{r1} = 1.0$; $\epsilon_{r2} = 2 - j$, $\mu_{r2} = 1.0$. The incident angle to the system is $\alpha = 45^\circ$ still. The figure shows the asymmetry of the system causes the asymmetry of the scattered field. The pattern for the lossy case is no longer similar to that for the lossless case just by some attenuation in amplitude. Newly deep attenuation points for the lossy pattern appear somewhere instead some old ones disappear.

IV. CONCLUSIONS

The iterative algorithm based on measured equation of invariance is proposed for the scattering problem of multiple cylinders for the first time. The iterative procedure in terms of matrix is derived. The present method is shown effective and convenient with no limitation on configuration and media for the problem.

REFERENCES

- [1] V. Twersky, "Multiple scattering of radiation by an arbitrary configuration of parallel cylinders," *J. Acoust. Soc. Amer.*, vol. 24, pp. 42–46, 1952.
- [2] C. R. Mullin, R. Sandburg, and C. O. Velline, "A numerical technique for the determination of scattering cross sections of infinite cylinders of arbitrary geometrical cross section," *IEEE Trans. Antennas Propagat.*, vol. AP-13, pp. 141–149, Mar. 1965.
- [3] N. Zitoron and S. N. Karp, "Higher order approximation in multiple scattering I: Two-dimensional scalar case," *J. Math. Phys.*, vol. 2, pp. 394–402, 1961.
- [4] K. Hongo, "Multiple scattering by two conducting circular cylinders," *IEEE Trans. Antennas Propagat.*, vol. AP-26, pp. 748–751, Sept. 1978.
- [5] J. W. Young and J. C. Bertrand, "Multiple scattering by two cylinders," *J. Acoust. Soc. Amer.*, vol. 58, pp. 1190–1195, 1975.
- [6] H. Ragheb and M. Hamid, "Scattering by N parallel conducting circular cylinders," *Int. J. Electromagn.*, vol. 59, pp. 407–421, 1985.
- [7] A. Z. Elsherbeni and M. Hamid, "Scattering by parallel conducting circular cylinders," *IEEE Trans. Antennas Propagat.*, vol. AP-35, pp. 355–358, Mar. 1987.
- [8] M. G. Andreasen, "Scattering from parallel metallic cylinders with arbitrary cross sections," *IEEE Trans. Antennas Propagat.*, vol. AP-12, pp. 746–754, Nov. 1964.
- [9] A. A. Kishk and L. Shafai, "Different formulations for numerical solution of single and multibodies of revolution with mixed boundary conditions," *IEEE Trans. Antennas Propagat.*, vol. AP-34, pp. 666–673, May 1986.
- [10] G. Mur, "Absorbing boundary conditions for the finite-difference approximation of the time-domain electromagnetic-field equations," *IEEE Trans. Electromagn. Compat.*, vol. EMC-23, pp. 377–382, Nov. 1981.
- [11] K. K. Mei, R. Pous, Z. Q. Chen, and Y. W. Liu, "The measured equation of invariance: A new concept in field computation," *IEEE Trans. Antennas and Propagat.*, vol. 42, pp. 320–327, Mar. 1994.
- [12] W. Hong, Y. W. Liu, and K. K. Mei, "Application of the measured equation of invariance to solve scattering problems involving penetrable medium," *Radio Sci.*, vol. 29, no. 4, pp. 897–906, 1994.
- [13] R. Pous, M. D. Prouty, and K. K. Mei, "Application of the measured equation of invariance to radiation and scattering by flat surfaces," in *IEEE AP-S Symp. Dig.*, Ann Arbor, MI, p. 540, July 1993.
- [14] M. D. Prouty, R. Pous, K. K. Mei, and S. E. Schwartz, "Application of the measured equation of invariance to transmission lines and discontinuities," *IEEE AP-S Symp. Dig.*, Ann Arbor, MI, p. 280, July 1993.

[15] J. Chen, W. Hong, and J. Jin, "An iterative measured equation technique for electromagnetic problems," *IEEE Trans. Microwave Theory Tech.*, vol. 46, pp. 25-30, Jan. 1998.



Jun Chen received the B.S. and the M.S. degrees in microwave telecommunication engineering from Xidian University (formerly Northwest Institute of Telecommunication Engineering), Xi'an, China, in 1991 and 1994, respectively, and the Ph.D. degree in radio engineering from Southeast University, Nanjing, China, in 1997.

From 1994 to 1997, he was a Research Assistant in the State Key Laboratory of Millimeter Waves, Southwest University, Nanjing, China. From 1997 to 1998 he was a Postdoctoral Research Fellow in the Department of Electrical and Computer Engineering, University of Illinois at Urbana-Champaign (UIUC). He worked on the theory of microwave networks, design of communication systems, stealth research, propagation prediction for mobile systems, and complex image theory. Since 1998 he has been with the Department of Computer Engineering, University of California at Santa Cruz (UCSC), as a Visiting Researcher. He has authored over 30 papers in international journals and conference proceedings. He is currently engaged in electrical modeling and design automation of very large scale integration (VLSI) circuits. His interests include RF design, numerical methods in computational electromagnetics, circuit and electromagnetic modeling for interconnects, and packages in VLSI circuits.

Wei Hong (M'92) received the B.S. degree from Zhenzhou Institute of Technology, Zhenzhou, China, in 1982, and the M.S. and Ph.D. degrees from Southeast University, Nanjing, China, in 1985 and 1988, respectively, all in electrical engineering.

Since 1988, he has been with State Key Laboratory of Millimeter Waves, Southeast University, Nanjing, China, where he is currently a Professor. In 1993 and 1995 he was a Visiting Scholar at the University of California at Berkeley and the University of California at Santa Cruz, respectively. His research interests include numerical methods for electromagnetic problem, electromagnetic scattering, antennas, interconnects in very large scale integration (VLSI) circuits, and microwave/millimeter-wave systems.